ISSN: 2977-4047

Journal of Life Sciences Research and Reviews

SCIENTIFIC Research and Community

Review Article

Open Access

Inflow Control Device with Electro-Hydraulic Control System

Abusal YA*, Prokofev AA, Ismakov RA, Gazizov RR and ALDwairi RA

Department of Oil and Gas Well Drilling, Ufa State Petroleum Technological University Kosmonavtov, Russian Federation

ABSTRACT

This article presents an in-depth exploration of the design, modeling, and control of an advanced inflow control device (ICD). Existing control systems for ICDs are analyzed, highlighting their key features and assessing their advantages and drawbacks. Based on this analysis, the development of a new ICD design is proposed incorporating an electro-hydraulic control system.

The mathematical description of the valve operation is provided, elucidating the principles behind its functioning. To simulate and evaluate the performance of the proposed ICD, a comprehensive model is built using Simulink, integrating a matrix approach and neural networks. The model enables the qualitative determination of the valve position based on the generated pressure drop, contributing to the optimization of the device's performance.

The article emphasizes the importance of automatically adjusting the actuator's position based on real-time measurements from various instruments. This enhances the efficiency and reliability of the ICD in dynamically controlling the flow rate in production wells. The use of a neural network-based approach aids in accurately determining the density of the flowing fluid and its impact on pressure drop, facilitating effective control strategies.

The results of their research are demonstrated, showcasing the successful operation of the developed ICD model. Through the use of 3D views and cross-sectional diagrams, the article provides a visual understanding of the ICD's components, including the overall device, central axis, and pressure sensor setting.

This article contributes to the advancement of inflow control devices by offering novel insights into their design, mathematical modeling, and control mechanisms. The findings pave the way for improved reservoir management, enhanced production optimization, and more efficient utilization of oil and gas resources.

***Corresponding author**

Abusal YA, Department of Oil and Gas Well Drilling, Ufa State Petroleum Technological University Kosmonavtov, Russian Federation.

Received: November 15, 2024; **Accepted:** November 24, 2024; **Published:** December 30, 2024

Keywords: Inflow Control Device, Electro-Hydraulic Control System, Mathematical Modeling, Simulation, Flow Rate Regulation, Reservoir Management, Production Optimization

Introduction

Intelligent well completion systems have been utilized in the oil and gas industry for several decades to address the challenge of managing fluid flow from reservoirs, especially in complex wells such as ERD, multilateral, or multibranch wells [1]. In the last decade, awareness of the need to use intelligent completion systems in the face of growing hard-to-recover oil reserves has increased dramatically. The demand for intelligent completion systems has significantly increased in recent years due to the rising importance of hard-to-recover oil reserves. Technological advancements in exploration and development have enabled the industry to target challenging geological and technical environments, necessitating the development of advanced intelligent completion tools. These tools should allow access to multiple zones at higher pressures and temperatures while minimizing costs and maximizing reliability [2].

Traditionally, intelligent completion systems consist of control and electrical lines, packers, permanent monitoring devices, inflow control devices, and control systems for the inflow control devices [3]. In recent years, the focus has shifted towards optimizing the control systems of inflow control devices and developing new designs for these devices, driven by advancements in technology and electronics [4]. Various control methods, including hydraulic and electric systems, have been developed and tested. Early systems relied heavily on electronics, but their reliability was limited by the available technology and susceptibility to leaks in electronic connections. Subsequently, hydraulic systems became the preferred choice due to their reliability, although they had certain limitations [5].

The limitations of the electronics available at the time were the primary cause of issues with these systems. Additionally, leaks in the electronic connections and lines often contributed to the problems. In order to address the reliability concerns, a shift was made towards systems that relied solely on hydraulics for control. However, this transition also imposed limitations on the system's capabilities [6]. Eventually, advancements were made to enable control over multiple zones using fewer hydraulic lines. Nevertheless, this led to an increased number of components, higher costs, and added complexity to the well completion process [7].

With the increasing popularity of smart completion systems and the need for enhanced zone control, there has been a renewed interest in incorporating electronics into well systems [8]. While

the reliability of electronic components has significantly improved, challenges remain regarding the protection of these components from well fluids [9]. The solution lies in designing systems that utilize robust and pressure-resistant electrical components [10].

Although hydraulic systems are traditionally favored in terms of reliability and cost-effectiveness, their control capabilities are limited, necessitating complex control systems to manage a higher number of controlled zones [11]. Consequently, control schemes incorporating electric or electro-hydraulic systems have gained popularity due to their ability to offer greater zone control with relatively simpler control system deployment [12].

This article addresses the need for an innovative design of an inflow control device that minimizes the drawbacks of both hydraulic and electro-hydraulic systems by incorporating minimal electronics and employing a channel and flow restrictor-based system to block the inflow channel. The hydraulic system is integrated directly into the device, eliminating the need for hydraulic lines typically found in traditional hydraulic and electro-hydraulic systems.

Design and Operation of the Electro-Hydraulic Inflow Control Device

To address these challenges, the design of the inflow control device must include two key areas: the fluid (mixture of oil, water, and gases) characterization area and the direct control area. Figure 1 provides a 3D view of the final assembly of the device, figure 2 shows a cross-section along the central axis, and figure 3 depicts a cross-section of the pressure sensor setting. The inflow control device consists of a housing 7 with main and secondary channels, throttle packages 1 and 2, flow restrictors 3, 4, 5, and 6, and components of the actuator assembly (damper 8, piston rod 9, threaded bushing 10, piston 11, spring 12, crosspiece 13, and nut 14). The housing is sealed by plugs 21 and 22. Throttle packages 1 and 2 are designed as assemblies comprising a body, a threaded nut, throttle washers, and inserts [13].

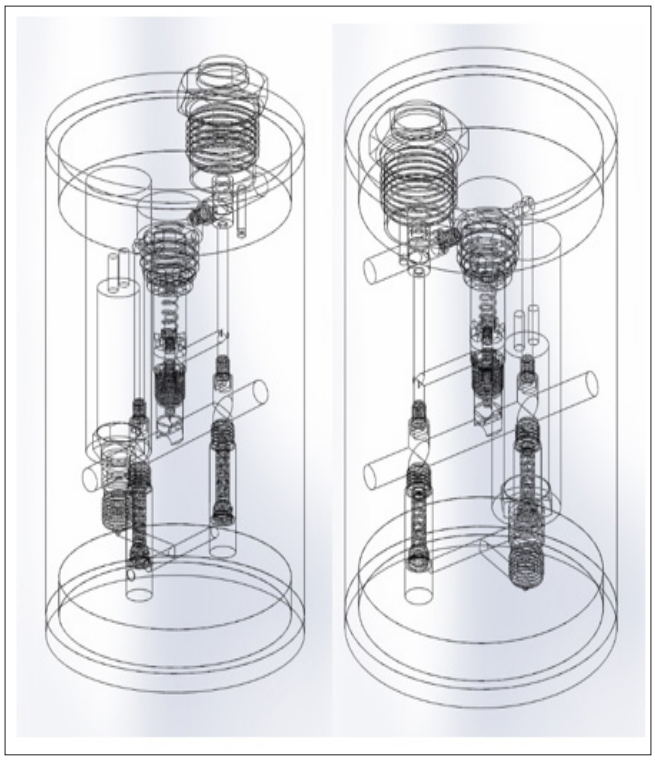

Figure 1: - 3D Visualization of the Inflow Control Device

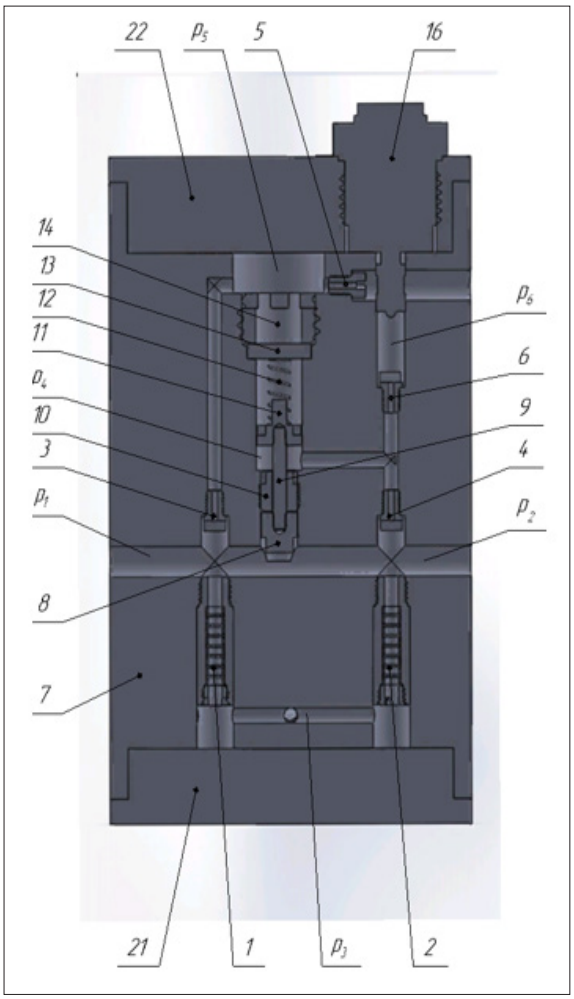

Figure 2: Cross-sectional View of the Inflow Control Device Along its Central Axis

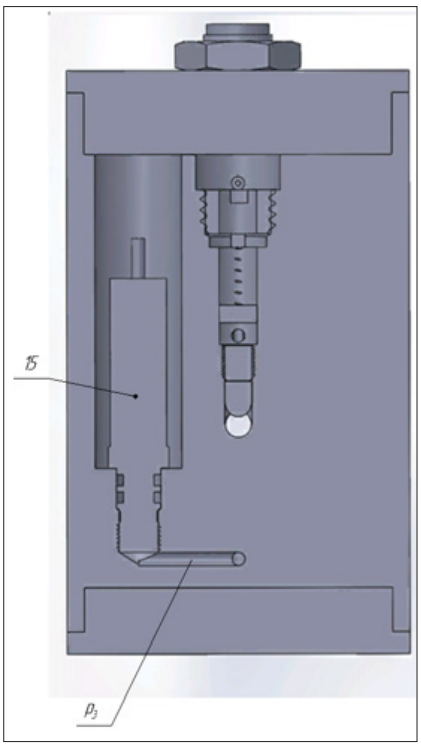

Figure 3: Cross-sectional View of the Pressure Sensor Setting

The inflow control device, along with other devices, is installed between the packers on the liner. It is lowered into the well so that the packers divide the wellbore into independent sections. Once the string is run, the packers activate and close off the selected intervals. The fluid flow passes through the main channel, allowing it to move from the reservoir into the production pipe. In the secondary channel, as the fluid passes through throttle packages 1 and 2, a pressure drop occurs, which is influenced by the density and temperature of the fluid. Figure 4 illustrates the schematic diagram of the throttle package, where the pressure drop can be adjusted by selecting the number of washers 19.

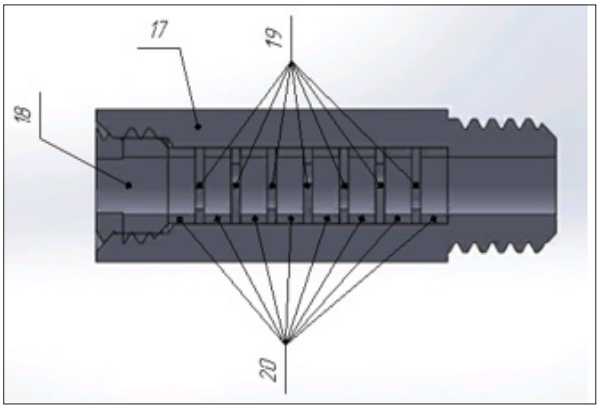

Figure 4: Throttle Package

To account for changes in fluid properties, specifically when a more viscous liquid like oil flows, the solenoid valve 16 is in an open state. However, when a less viscous liquid such as gas or water flows, the pressure increases, triggering a change detected by the pressure sensor 15. Depending on this difference, the position of the actuator's damper 8 changes. The solenoid valve 16, driven by an automatic control system from the wellhead, allows for the adjustment of the damper's position. When a change in fluid is detected by the pressure sensor 15, the solenoid valve 16 closes or opens. Upon closing, the pressure above the piston 11 increases, moving the damper 8 downward and blocking the main channel.

Mathematical Description of the Inflow Control Device's Operation
To evaluate the performance of the inflow control device, a model was developed in the Simulink simulation environment. This model utilizes a matrix approach and neural networks to establish a qualitative relationship between the actuator's position and the generated pressure drop. Transfer functions were then obtained based on the Laplace transform to control the actuator. Statistical calculations were conducted to accurately adjust the pressure drop dependence on the density of the incoming liquid, considering the coefficient of volumetric expansion that is influenced by the fluid's temperature.

The pressure drop depends on the density, temperature, and velocity of the incoming fluid. The fluid flow rate through the flow restrictors can be determined using equation 1, which considers various factors such as acceleration of gravity, fluid density, viscosity, flow restrictor area, and inlet/outlet pressures.

$$Q=a\cdot\mu\cdot f\cdot\sqrt{(P_{in}-P_{out})} \qquad (1)$$

where $a=\sqrt{\frac{2g}{\rho}}$;

g – acceleration of gravity, m/s^2;
ρ – density or specific gravity of a fluid flow, kg/m^3 ;
μ – drag coefficient;
f – flow restrictor area, m^2;
P_{in} – inlet pressure, Pa;
P_{out} – outlet pressure, Pa.

The control of the inflow control device involves considering the forces acting on the piston. These forces include the pressure drop across the device, the hydraulic pressure acting on the piston, and any external forces or constraints. By analyzing these forces, we can determine the appropriate control actions required to achieve the desired flow rate. Equation 2 describes the balance of forces acting on the piston, taking into account mass, spring constant, preload force, and area under the piston.

$$m_{\Sigma}\ \ddot{x}+C_{пр}\ x+R_{пр}=F_{п}\ (P_5-P_4), \qquad (2)$$

where m_{Σ} – total mass of the actuator and piston, kg;

$C_{пр}$ – spring constant, N/m;
$R_{пр}$ – preload force on the piston, N;
$F_{п}$ – area under the piston, m^2;
P_5 – pressure above the piston, Pa;
P_4 – pressure under the piston, Pa.
low rates through the flow restrictors Q_3 and Q_4 are calculated using equations 3 and 4, respectively.

$$Q_3 = a\mu f_3\sqrt{P_1-P_5} = a\mu f_{сл}\sqrt{P_5-P_{сл}} + F_{п}\dot{x}, \qquad (3)$$

$$Q_4 = a\mu f_4\sqrt{P_2-P_4}, \qquad (4)$$

The total flow rate Q after the damper is determined by equation 5.

$$Q = a\mu f_{п}\sqrt{P_1-P_2} + Q_4 + Q_2, \qquad (5)$$

By considering a small displacement of the piston X, we can approximate the equation using linearization techniques. This approximation allows us to simplify the equation and analyze the behavior of the system around a specific operating point utilizing equation 2:

$$m_{\Sigma}\ \Delta\ddot{x}+C_{пр}\ \Delta x=F_{п}\ (\Delta P_5-\Delta P_4), \qquad (6)$$

Referring to equation 1, we can derive the equations governing the flow rate of the liquid as it passes through the flow restrictors. These equations are as follows:

$$\Delta Q_1=\alpha_1\ (\Delta P_1-\Delta P_3), \qquad (7)$$

where $\alpha_1 = \frac{a\mu f_1}{2\sqrt{P_1-P_3}}$ – linearization factor

$$\Delta Q_3 = \alpha_3(\Delta P_1-\Delta P_5) = \alpha_3\cdot\Delta P_5 + F_{п}\Delta\dot{x}, \qquad (8)$$

$$\Delta Q_4 = \alpha_4(\Delta P_2-\Delta P_4), \qquad (9)$$

$$\Delta Q_4 + \Delta Q_6 = F_{п}\Delta\dot{x} \qquad (10)$$

By assuming that $P_6 \approx P_4$, we can simplify the equations as follows:

$$\Delta Q_6 = \alpha_6 \Delta P_4 \quad (11)$$

By considering the assumption 11, we can solve equations 9 and 10 as follows:

$$\alpha_4 \Delta P_2 + (\alpha_6 - \alpha_4)\Delta P_4 = F_п \Delta \dot{x} \quad (12)$$

Since we can assume $\Delta P_2 \approx 0$, we can simplify the equations and find:

$$\Delta P_4 = \frac{F_п}{\alpha_6 - \alpha_4} \cdot \Delta \dot{x} \quad (13)$$

From equation 8, assuming $\Delta P_1 \approx 0$, we can find ΔP_5:

$$\Delta P_5 = \frac{F_п}{\alpha_5 - \alpha_3} \cdot (-\Delta \dot{x}) \quad (14)$$

By substituting the obtained dependencies into the piston displacement equation 6, we can derive the balance of forces:

$$m_\Sigma \Delta \ddot{x} + \left(\frac{F_п^2}{\alpha_5 - \alpha_3} + \frac{F_п^2}{\alpha_6 - \alpha_4}\right)\Delta \dot{x} + C_{пр}\Delta x = 0 \quad (15)$$

The resulting equation corresponds to the dynamics of the damper and can be represented as the equation of an oscillatory link:

$$W(s) = \frac{K}{T^2 S^2 + 2\xi T s + 1}, \quad (16)$$

where $T = \sqrt{\frac{m}{C_{пр}}}$ – transient time;

$K = \frac{\Delta x}{\Delta P_3}$ – transmission ratio;

ξ – attenuation parameter in the range $0 < \xi < 1$

To account for the variable α_{ij} (linearization coefficient) and the equations of the transfer attenuation degree and time constant in equation 15, it is recommended to utilize a matrix approach for constructing the model. This approach involves conducting static calculations to determine the relationships between pressure drop, temperature, and liquid density. By obtaining a single calculated point, the matrix approach can be employed to build the model effectively.

Static Valve Operation Calculations

During the static valve operation calculations, actual production well parameters and proposed design parameters of the inflow control device were taken into consideration. It was crucial to ensure that the condition $P_6 > P_4$ is satisfied for the system to function properly. By incorporating these data, the static calculations were performed to evaluate the performance of the valve.

To determine the degree of damping ξ of the process, the following equation was employed:

$$2\xi T = \frac{F_п^2}{C_{пр}}\left(\frac{1}{\alpha_5 - \alpha_3} + \frac{1}{\alpha_6 - \alpha_4}\right)$$

The linearization coefficients and the time of the transient process were determined using the following formulas:

$$\alpha_4 = \frac{a\mu f_4}{2\sqrt{P_2 - P_4}};$$

$$\alpha_5 = \frac{a\mu f_5}{2\sqrt{P_5 - P_6}};$$

$$\alpha_{сл} = \frac{a\mu f_5}{2\sqrt{P_6 - P_4}};$$

$$T = \sqrt{\frac{m}{C_{пр}}}$$

By applying equation 17, the degree of damping was found to be $\xi = 0.000898808$, indicating that the process is damped ($\xi < 1$).

To investigate the relationship between the pressure drop across the throttle package and the density of the incoming liquid, equation (1) was utilized, and a corresponding graph (Figure 5) was constructed.

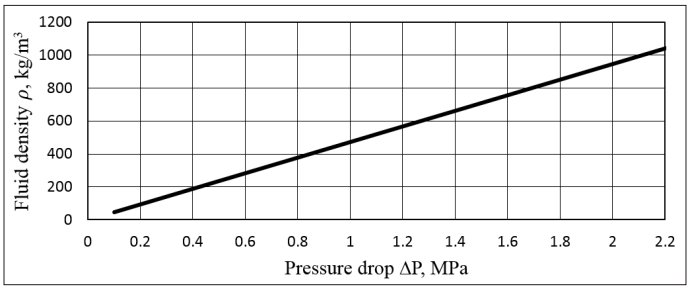

Figure 5: The Relationship Between the Pressure Drop and the Density of the Incoming Liquid

To account for the decrease in density of the water-oil emulsion with increasing temperature, correction factors were determined using the formula:

$$\beta_t = \frac{1}{\rho_0} \cdot \frac{\Delta \rho}{\Delta t},$$

where β_t is the coefficient of volumetric expansion, which quantifies the relative change in volume for a 1 °C temperature variation. To incorporate the temperature effect on the density of the incoming liquid, volume expansion coefficients were computed across a temperature range of 0 to 180 °C. By considering the volume expansion coefficient β_t, a plot was generated, illustrating the relationship between the pressure drop and the density of the incoming liquid. This plot, depicted in figure 6, accounts for the influence of the volume expansion coefficient on the pressure drop, providing insights into how temperature affects the density of the liquid and subsequently impacts the system dynamics.

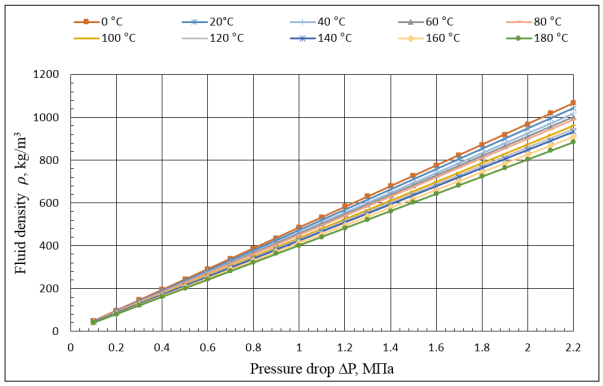

Figure 6: The Relationship Between the Pressure Prop and The Density of Incoming Liquid with Temperature Stratification

Simulation in Simulink

The model of the inflow control device operation was constructed in Simulink using neural network blocks, logical control blocks for conditional actions, and transfer function blocks representing the derived transfer functions based on calculated data in the form of polynomial ratios. Figure 7 illustrates the built model of the inflow control device in Simulink [14].

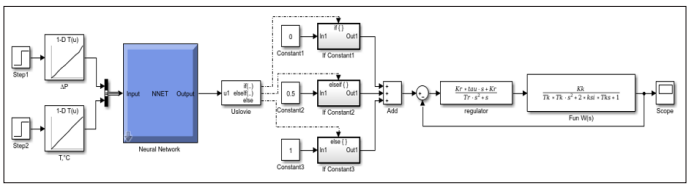

Figure 7: Model of the Inflow Control Device in Simulink

To determine the density values based on the pressure drop and temperature, a neural network was implemented using the Neural Network Toolbox, an extension package in MATLAB. This toolbox enables the accurate representation of transient processes, specifically through the matrix representation method of dynamic characteristics. The dynamic characteristics method captures the relationship between three parameters: pressure drop after the flow restrictor, liquid density, and temperature. The approach involves defining the parameters of dynamic characteristics in the form of matrices. In this model, the input consists of two parameters: the pressure drop after the throttle package and the fluid temperature. These values are used to determine the corresponding density of the liquid.

To create a comprehensive model encompassing the entire range of possible values for the three parameters, the matrix representation method of dynamic characteristics was employed. This approach resulted in the derivation of a pressure drop matrix with the following structure:

$$A_{\overline{\Delta P}} = \begin{pmatrix} \Delta P_1 & T_1 & \rho_1 \\ \Delta P_1 & T_1 & \rho_1 \\ \vdots & \vdots & \vdots \\ \Delta P_i & T_j & \rho_m \end{pmatrix}.$$

To construct the matrix, constant pressure drop values were determined and utilized. For each pressure drop value, the corresponding temperature and density values were inputted into the matrix based on the information presented in figure 6.

The density value is inputted into the conditional operator block (Uslovie), along with the subsystems (If Constant), to determine the valve position. The logic for setting the parameters of the block is illustrated in figure 8.

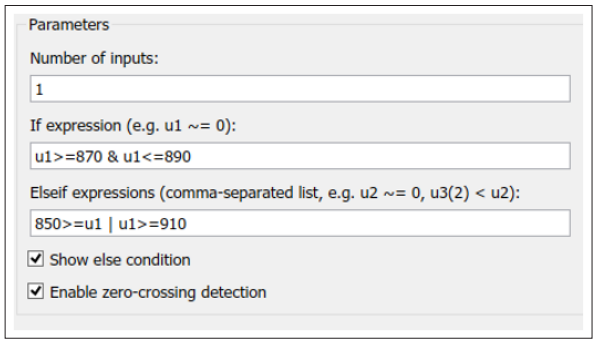

Figure 8: The logic of the "Uslovie" Operator

The "Uslovie" operator in the model is configured to have a specific number of inputs, which, in our case, is one input parameter representing the density obtained from the neural network model (Neural Network). The operator evaluates a conditional expression (If-expression) to determine whether it should execute. In the conditional expression, the condition for execution is defined using the parameter u1, which represents the density. If the condition evaluates to true, a control signal is generated at the "if" output port.

In addition to the main expression, the "Uslovie" operator can include alternative conditions (Elseif-expressions) that are executed only if the main expression evaluates to false. The number and parameters of these alternative conditions can be modified according to the desired quantities and possible valve positions in the system. When any of the conditions evaluates to true, a control signal is fed into the "if" input of the subsystems (If Constant), and the output of the subsystem represents the value of the constant located at its input (In). In this case, the values 0, 0.5, and 1 correspond to 0%, 50%, and 100% valve opening, respectively.

After setting the operating conditions, the transfer function of the valve controller W(s) was determined using equation 16. The values of the transition period time $T_k = 0.037$ s and the damping degree $\xi = 0.000899$, obtained during the static calculations, were utilized in this process.

The transfer function coefficients of the valve K_k and the regulator K_r are selected based on the consideration that their sum should equal 1 ($K_k + K_r = 1$). By satisfying this condition, the coefficients were determined as follows:

$K_k = 0.9$;

$K_r = 0.1$;

$tau = 1$;

$T_r = 1.1$.

With the help of transfer function blocks (regulator) and (FunW(s)), the transfer function of the damper and valve was set as a ratio of polynomials. Figure 9 illustrates the final result of the simulation at the output of the model.

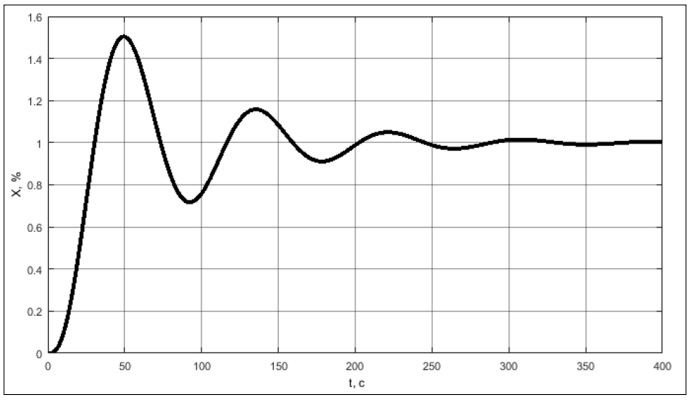

Figure 9: Simulation Result

The simulation resulted in establishing the transient process within a time frame of t = 300 s, which is considered adequate for such systems. This indicates that the system is functioning properly. The transient process within the given time period will not significantly impact the extraction of reserves from the well itself, as its duration is considerably shorter compared to the processes occurring in the well.

Conclusion

During the analysis of existing control systems for inflow control devices, several key features were identified and evaluated.

Positive aspects and limitations were identified, leading to the development of new inflow control devices utilizing an electro-hydraulic control system. This analysis served as a foundation for the development of a new design scheme for the inflow control device, enabling automatic adjustment of the actuator position based on measurement data.

The mathematical description of the valve operation was provided, outlining the principles underlying its functionality. Subsequently, a valve model was created within the Simulink simulation environment, utilizing a matrix approach and neural networks. This model aimed to establish a qualitative relationship between the valve position and the generated pressure drop. The neural network block and the simulation results are presented, demonstrating the effectiveness of the developed model.

Overall, this work encompasses a comprehensive approach, combining analysis, mathematical modeling, and simulation to enhance the performance and control of inflow control devices. The results contribute to the advancement of efficient and automated control systems in oil and gas production.

References

1. Li Z, Fernandes P & Zhu D (2011) Understanding the Roles of Inflow-Control Devices in Optimizing Horizontal-Well Performance. SPE Drilling & Completion 26: 376-385.
2. Second Generation Interval Control Valve (ICV) (2023) Enhances Operational Efficiency and Inflow Performance in Intelligent Completions | IADC/SPE Asia Pacific Drilling Technology Conference and Exhibition https://onepetro.org/SPEAPDT/proceedings-abstract/12APDT/All-12APDT/SPE-153700-MS/155740.
3. Shaw J (2011) Comparison of Downhole Control System Technologies for Intelligent Completions. Presented at the Canadian Unconventional Resources Conference, OnePetro https://doi.org/10.2118/147547-MS.
4. Jacob S, Abdulbaqi N, Verma C, Younes R (2016) Case Study of Intelligent Completion with New Generation Electro-Hydraulic Downhole Control System. Presented at the SPE Kingdom of Saudi Arabia Annual Technical Symposium and Exhibition, OnePetro https://doi.org/10.2118/182761-MS.
5. Huiyun M, Chenggang Y, Liangliang D, Yukun F, Chungang S, et al. (2020) Review of intelligent well technology. Petroleum 6: 226-233.
6. Hodges S, Olin G, Sides W (2000) Hydraulically-Actuated Intelligent Completions: Development and Applications. In All Days (p. OTC-11933-MS). Houston, Texas: OTC. https://doi.org/10.4043/11933-MS.
7. Ajayi A, Oluwatosin A, Fasasi T, Giuliani C, Smith R, et al. (2009) Surface Control System Design for Remote Wireless Operations of Intelligent Well Completion System: Case Study. In All Days (p. SPE-121710-MS). Amsterdam, The Netherlands: SPE.
8. Garcia E & Saldanha S (2016) Electrohydraulic ICV Control System: A Novel Approach to Multizonal Control https://doi.org/10.4043/26816-MS.
9. Hsieh L (2017) Intelligent completion advances target improved reliability in HPHT conditions, simplified deployment https://drillingcontractor.org/intelligent-completion-advances-target-improved-reliability-in-hpht-conditions-simplified-deployment-44051.
10. Wang J, Zhang N, Wang Y, Zhang B, Wang Y, et al. (2016) Development of a downhole incharge inflow control valve in intelligent wells. Journal of Natural Gas Science and Engineering 29: 559-569.
11. Robinson M (2003) Intelligent Well Completions. Journal of Petroleum Technology 55: 57-59.
12. Zeng Q, Wang Z, Wang X, Li Y, Zou W, et al (2014) A Novel Autonomous Inflow Control Device Design: Improvements to Hybrid ICD. https://doi.org/10.2523/IPTC-17776-MS.
13. Prokofev AA, Ismakov RA, Chizhov AP, Gazizov RR (2023) Well fluid inflow control device, patent number: RU2798005C1, https://www.fips.ru/registers-doc-view/fips_servlet?DB=RUPAT&DocNumber=2798005&TypeFile=html.
14. Ismakov RA, Denisova EV, Chernikova MA, Sidorov SP (2019) System of device for controlling fluid injection in a well. Bulletin of the Tomsk Polytechnic University. Geo Assets Engineering 330: 192-198.

Copyright: ©2024 Abusal YA, et al. This is an open-access article distributed under the terms of the Creative Commons Attribution License, which permits unrestricted use, distribution, and reproduction in any medium, provided the original author and source are credited.